https://doi.org/10.46813/2024-151-060

IMPROVING THE FUNCTIONALITY OF THE SMALL-DIMENSION ACCELERATOR DIN-2K WITH A PLASMA OPENING SWITCH

D.V. Vinnikov[1,2], V.V. Katrechko[1], O.V. Manuilenko[1,3], O.M. Ozerov[1], I.N. Onishchenko[1], V.I. Tkachev[1], V.B. Yuferov[1], S.V. Marchenko[1]
[1]NSC "Kharkov Institute of Physics and Technology", Kharkiv, Ukraine;
[2]O.Ya. Usikov Institute for Radiophysics and Electronics, Kharkiv, Ukraine;
[3]V.N. Karazin Kharkiv National University, Kharkiv, Ukraine
E-mail: vinniden@gmail.com

Experimental studies were carried out to establish the effect of the parameters of various components of an electronic accelerator with an IES cell and a POS on the values of the current and the power of the accelerated beam. The studies were focused on the choice of the parameter ratio for the discharge circuit of the inductive energy storage cell, geometric shape and material of the cathode, size of the anode-cathode gap and dielectric inserts. The established optimal set of the specified parameters made it possible to obtain a pulsed electron beam with a duration of 200 ns, a current of 30 kA and a power of 6 GW.

PACS: 52.75.−d, 94.20.wc, 52.80 Vp, 52.70Kz, 29.30Ep

INTRODUCTION

The direct-action electronic accelerator equipped with the inductive energy storage (IES) cell and plasma opening switch (POS) is used for those application fields that require small overall dimensions and appropriate weight characteristics of the accelerator that ensure its maneuverability and the possibility of placement on flying platforms.

Earlier [1–5], we used a DYN-2K accelerator for the experimental studies of the physical processes of the formation of a plasma bridge by using several plasma guns and its rupture in the discharge circuit of an IES cell accompanied by an induced multiplication of the voltage on the cathode of a vacuum diode. The resulting explosive emission of plasma on the cathode and the accelerating field in the cathode-anode gap made it possible to form a pulsed electron beam. Physical processes, including the dynamics of the plasma current switch, are discussed in detail in theoretical research papers [6–10].

The purpose of this research was to improve the functionality of the DYN-2K accelerator by increasing its power and transporting the beam with minimum losses due to the optimal selection of the parameters of the accelerator components, in particular the ratio of the parameters of the discharge circuit of the IES cell, the geometric shape, the material of cathode, and also the size of the anode-cathode gap and the use of dielectric inserts.

1. DIAGNOSTICS

The operation procedure, the parameters of the electric circuit of the accelerator and the diagnostic equipment are described in detail in papers [1, 11]. Oscilloscopes were used as analog-to-digital converters (ADCs), in particular 4-channel OWON XDS3104E with a bandwidth of 100 GHz and a sampling rate of 1 GSa/s; 4-channel Siglent SDS 2204X, 200 MHz, 2 GSa/s; 4-channel Agilent infinium 54855A DSO, 6 GHz, 20 GSa/s.

Fig. 1 shows a general view of the accelerator with its equipment, vacuum system and diagnostic tools.

The upgraded high-voltage insulation of the step-up transformers enabled the increase in the charging voltage up to 45 kV for the pulse current generator (PCG) and to 18 kV for plasma guns.

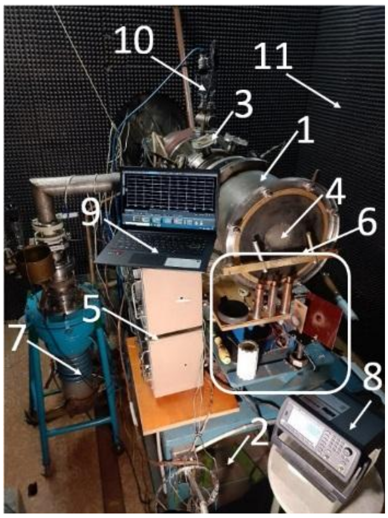

Fig. 1. Photo of the electron accelerator: 1 is the accelerator chamber body; 2 is high-voltage accumulators; 3 is plasma guns; 4 is insulating flange; 5 is vacuum gauges; 6 is vacuum diode equipment set; 7 is steam-oil vacuum pump; 8 is the generator of nanosecond pulses; 9 is portable diagnostic equipment with software; 10 is thermocouple and ionization vacuum lamps; 11 is noise-absorbing plates

In addition, to determine the power of the beam, a capacitive voltage divider was manufactured, mounted and calibrated, the division factor of which depends on the gap between the high-voltage and low-voltage arms and it was equal to k = 1886, with a distance of 60 mm between the plates of the high-voltage arm of the divider, and about 4 μm between the plates of the low-voltage arm.

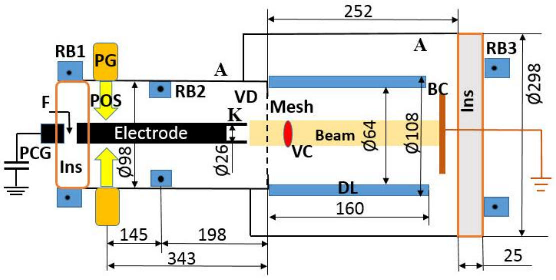

Fig. 2. DIN-2K direct-action electron accelerator circuit. A is the accelerator chamber body, anode; K is the tubular cathode mounted on a rod; Mesh is the anode mesh; DI is the dielectric insert; POS is the plasma opening switch or plasma current switch; Beam is the electron beam; VC is the virtual cathode; PCG is the pulse current generator; PG is plasma guns; VD is the vacuum diode, i.e. the electron acceleration gap; BC is the beam collector; F is the air trigatron; RB1–RB3 are Rohovsky belts; Ins is a vacuum insulator made of organic glass

The conditions under which cathodes were studied and optimal geometry was determined to obtain maximum beam currents (Ibeam), break currents (Ibreak) and maximum current in the primary circuit of the PCG-POS (Imax) were as follows: the diameter of the anode was unchanged and it was equal to 298 mm. The cathode-to-anode mesh distance was 6 mm. The anode mesh was made of stainless steel with a geometric transparency of 65%, and the mesh size was 1x2 mm. The distance from the anode mesh to the current receiver was 30 mm. The diameter of the ring on which the anode mesh was fixed was 100 mm, and the thickness was 10 mm. The diameter of the grid itself was 80 mm. The main dimensions are shown on Fig. 2.

The introduced technical changes of the accelerator allowed us for the first time to increase the operating voltage at the PCG from a maximum of 30 to 45 kV, and to ensure the operation of PG at voltages exceeding 12 kV, up to 18 kV inclusively.

During the experiment, the PCG voltage varied from 25 to 45 kV, with a step of 5 kV, and the voltage on the PG from 10 to 16 kV. The delay time was fixed and it was 3 μs. It has been experimentally determined that the time delay within 6 μs is optimal. The optimality was determined by the moment and magnitude of the interruption of the current flowing in the PCG-POS loop and by the beam current value.

The main types of cathode geometries are shown in Table 1.

Table 1

	
Copper electrode in the form of the expanding cone	
	
Copper electrode in the form of a gear	
	
Electrode in the form of the hollow tube made of steel	
	
Electrode in the form of graphite disc	

General view of some dielectric inserts are given in Table 2.

Table 2

	
Dielectric insert in the form of the porcelain isolator	
	
Carbon dielectric insert	

Photodiode sensors were mounted to ensure the measurement of the propagation speed of plasma created by plasma guns along the axis and radially. The set speed was (0.5…5)·10^6 cm/s, and the plasma gun voltages varied in the range of 10 to 16 kV [11]. Taking into account the distance from the plasma source to the anode mesh of 343 mm, it can be stated that the plasma fails to spread into the beam formation zone before the formation of explosive emission, reducing thus beam losses due to the existing time delay between the activation of the plasma guns (PG) and the operation of the PCG of no more than 4 μs.

To determine the level of electromagnetic interference, antennas of pin and ring types and Hertz dipoles were installed in different parts of the absorbing chamber. A horn with cut-off frequencies of 2.027 GHz was also used to determine the intensity and presence of the microwave component of the total radiation. It was established that the intensity of microwave interference is at least 5 times lower than that of the radiation of the kilohertz and megahertz range, and it does not affect the properties of the investigated signals.

In order to improve the output characteristics of the accelerator, changes were made in the power supply system of the plant, the technological implementation of the vacuum diode system and electron beam transportation system.

2. EXPERIMENTS

2.1. CURRENT MEASUREMENT AND ELECTRON BEAM ENERGY ESTIMATION

The beam current and induced voltages were measured to determine the power of the beam. Fig. 3 shows the maximum current (Imax) in the vacuum diode with the POS momentum, the residual current (Iresidual) and the beam current (Ibeam) injected from the end of the cathode in the direction of the anode mesh and further into the vacuum space.

The delay time was 3 μs, the charging voltage of the PCG was 45 kV, and the gun voltage was 12 kV. The maximum current on the diode was 96 kA. The beam current was 10.5 kA, recorded at a distance of 30 mm from the anode mesh.

To determine the beam current in the region before its interaction with the mesh and to determine losses, the beam collector was placed instead of the mesh at the mesh position.

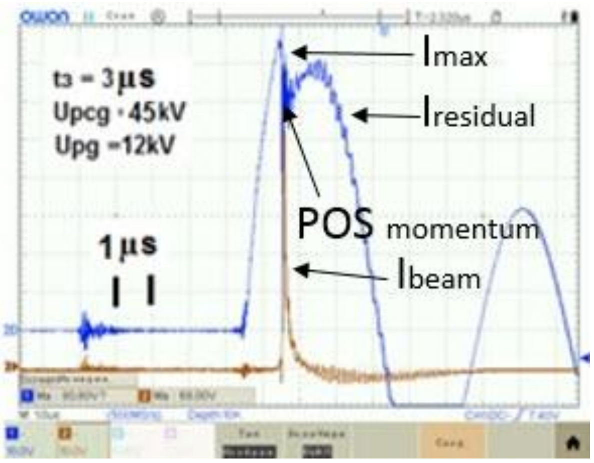

Fig. 3. A typical oscillogram of the current opening mode with simultaneous fixation of the current beam

The induced voltage on the vacuum diode for the indicated parameters of the discharge circuit was 182 kV (Fig. 4) and it corresponds to the voltage multiplication factor of K=4.

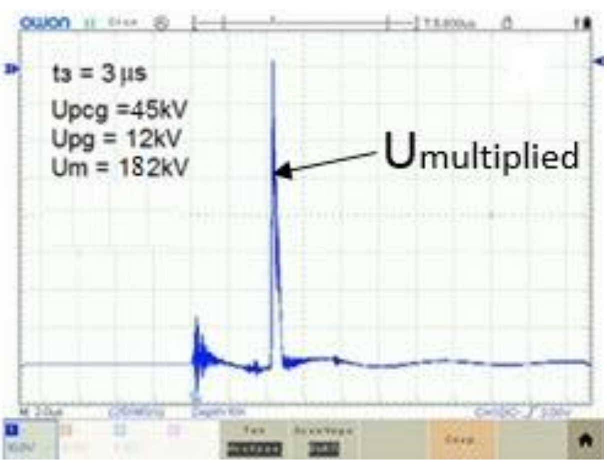

Fig. 4. Oscillogram of the voltage pulse in the cathode-anode gap

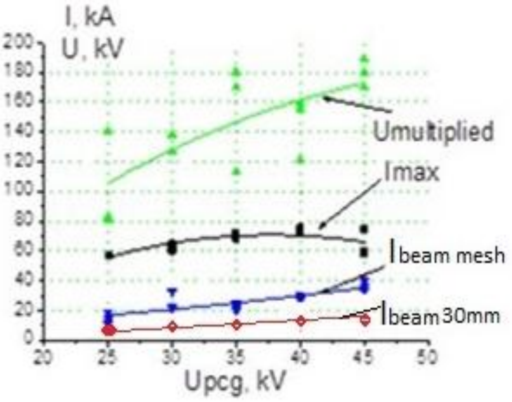

Fig. 5. Dependence of an induced voltage a maximum current before the POS opening and the beam current on the PCG voltage, for the case when the current sensor is placed instead of the anode mesh at a distance of 30 mm from the mesh

Fig. 5 shows that the beam current before the mesh is on average 2.7 times higher than the beam current after it, depending on the PCG charging voltage. At the same time, a maximum current on the vacuum diode before the opening of the plasma switch is the same in both cases and it reaches the values of 60 to 80 kA for the PCG charging voltage varying in the range of 25 to 45 kV. The induced voltage is almost linearly dependent on the PCG voltage, with the multiplication factor ranging from 3.3 to 5.2.

2.2. THE CHOICE OF THE GEOMETRY OF THE CATHODE TO OBTAIN A MAXIMUM BEAM CURRENT

The dependence of the beam current on the PCG charging voltage for different types of cathode geometry is shown in Figs. 6 and 7. Consideration is given to the five types of geometries of electrodes made of copper: a hollow copper tube, an expanding cone, a narrowing cone, electrodes in the form of a crown and a gear (some of them are presented in Table 1).

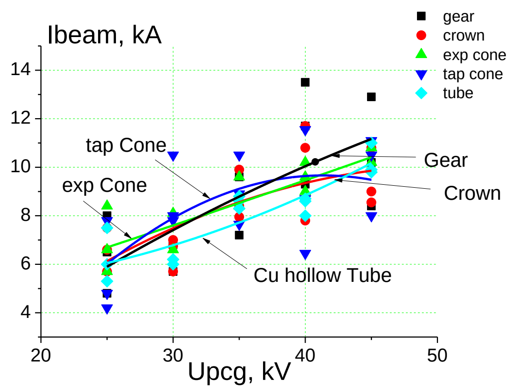

Fig. 6. Dependence of beam currents on the geometry of copper cathodes at different PCG charging voltage

The current of the beam Ibeam for all types of cathodes is characterized by a slow increase in the range of 3 to 11 kA. It can be seen that there is no significant difference in the values of the beam current for the selected types of geometries, at least up to the values of the PCG charging voltage of 40 kV. In the voltage range of 40 to 45 kV, preference can be given to the gear-shaped electrode, and it can be related to the presence of a larger number of areas with electric field inhomogeneity as compared to other geometries.

Carbon, steel and copper tubular electrodes and additionally a disc-shaped carbon electrode with a diameter equal to the diameter of the anode of 100 mm have been compared. Despite the higher values of Imax and Ibreak, the beam current for the disc-shaped cathode was at least two times lower compared to that of tubular electrodes, and it can be a consequence of the mismatch of the impedance of the vacuum diode, which depends on the geometry of the cathode, with the high-voltage pulse supplied from POS to the cathode, i.e. the anode gap of the vacuum diode. No significant difference in beam current values was observed for the three types of electrode materials.

For more accurate experimental estimation of the beam current, the beam collector was placed at the position of the anode mesh. Electrical short – circuit with the cathode was provided only after an electron beam was formed and electrons from the cathode hit the collector surface, as a result of explosive emission.

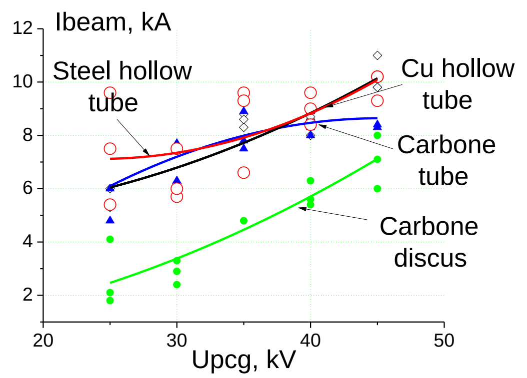

Fig. 7. Dependence of beam currents on the geometry of cathodes of different geometries and materials at different PCG charging voltages

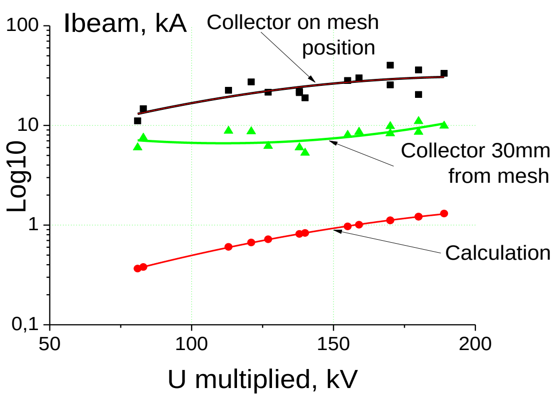

Fig. 8. Dependence of the beam current on the induced voltage in the cathode-anode gap for two options of the arrangement of the current collector and verification of the obtained data according to the "3/2 law"

Comparison of the current values for the geometry with a beam collector used instead of the anode mesh with the current when the anode mesh is placed at a distance of 6 mm from the cathode, and the beam collector is at a distance of 30 mm from the mesh and the calculation curve are shown in Fig. 8.

Beam current in Fig. 8 reaches 33 kA and is higher than the current recorded with the same parameters of the primary electric circuit, but for the case when the beam collector is at a distance of 30 mm from the anode mesh. It is indirectly indicative of the partial divergence of the beam electrons, which also indicates the influence of the anode field.

The verification calculation of the current was carried out according to the "3/2 law" of Child-Langmuir that has the following generalized form, for the anode with zero transparency:

$$I_{beam}(U) = 2.33 \cdot 10^{-6} U^{3/2}_{multiplied} S / d^2 ,$$

where I_{beam} is the beam current; $U_{multiplied}$ is the voltage induced in the cathode-anode gap; S is the cathode area; d is the distance between the cathode and the anode. Fig. 8 shows that the calculated and experimental curves differ under different initial conditions, by approximately 6 to 10 times depending on the location of the beam collector. These discrepancies are explained by the fact that the "3/2 law" considers a one-dimensional stationary model, that already has an error. This problem is disclosed in papers [12, 13]. However, it is important that the voltage dependence is preserved.

2.3. DEPENDENCE OF THE BEAM CURRENT ON THE SIZE OF THE CATHODE-ANODE GAP

In order to determine the dependence of the beam current on the distance of the cathode from the anode mesh, the structure design with a mobile mesh was created and used to ensure the prompt acquisition of the necessary data without violating the vacuum conditions. Fig. 9 shows the dependence of the beam current on the PCG charging voltage for different gaps between the cathode and the anode mesh.

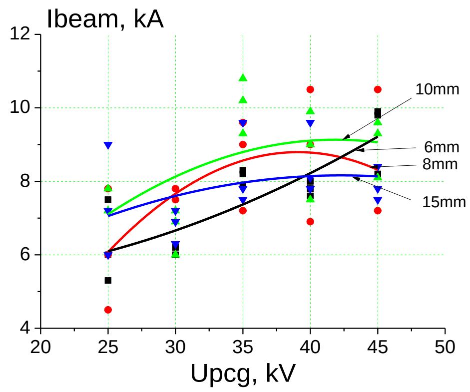

Fig. 9. Dependence of the beam current on the PCG charging voltage for different interelectrode gaps of the vacuum diode

The beam current was measured using a beam collector arranged at a distance of 30 mm from the anode mesh. The optimal gap was 10 mm. For this gap, the largest beam currents of 8.3 kA on average were obtained under all initial conditions. Whereas, for example, a gap of 6 mm had average values of about 7.5 kA.

Hence, it is shown that the output parameters of the accelerator can be changed and improved not only due to the charging voltage of the accelerator sources and the delay time, but also due to the shape of the cathode and the change in the cathode-anode gap of the vacuum diode.

2.4. THE EFFECT OF A DIELECTRIC FOCUSING LENS ON THE BEAM CURRENT

Based on the previous experiments that demonstrated a rather high angular spread of the electron beam and the associated losses, several types of dielectric focusing lenses were tested to reduce the losses of beam electrons.

The goal was to provide the focusing of the electron beam and reduce the loss of charge carriers. Focusing occurs due to the accumulation of electrostatic negative charge on the surface. Experiments were carried out for different cylinder diameters of dielectric inserts, in particular 30, 40, 65, and 150 mm at a fixed distance of 150 mm (Fig. 10). Some of the dielectric inserts are shown earlier in Table 2.

The optimal size of the dielectric focusing lens made of porcelain was established, and it was equal to 65 mm. It is closest to the actual diameter of the cylindrical anode, and at the same time it makes it difficult for electrons to exit from the vacuum diode along the radius, i.e. a free space for the exit of electrons can be considered as unavailable.

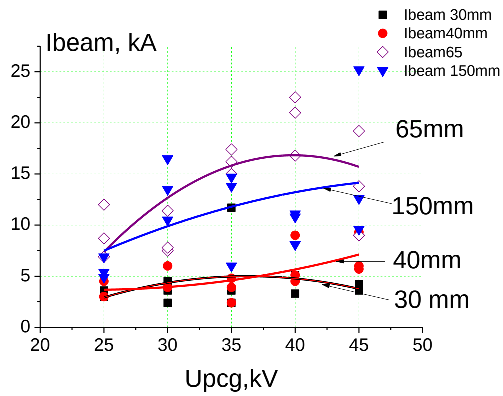

Fig. 10. Dependence of the beam current on the PCG charging voltage for different diameters of the dielectric tube

In cases where the diameter of the dielectric is commensurate with the radius of the cathode, or larger than the radius of the anode, there is a free space that can be entered by the beam electrons scattering through it.

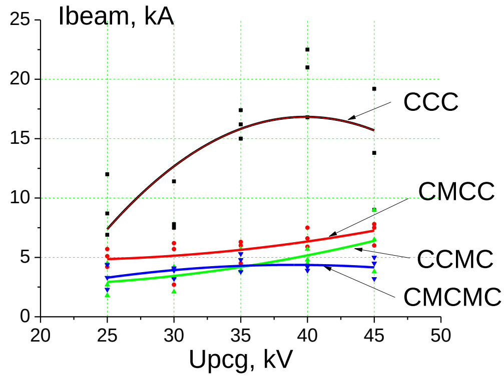

Fig. 11. Dependence of the beam current on the PCG charging voltage for different options of the location of the dielectric focusing lens

The influence of the mesh location relative to the dielectric lens and the number of meshes on the beam current has been determined. The experiment was carried out using a lens with a diameter of 65 mm. The beam collector was located at a distance of 30 mm from the end of the vacuum diode structure with a focusing lens.

The first type of the geometry of the vacuum diode is represented in the sequence of cathode – dielectric focusing lens in the form of a cylinder – beam collector or CCC – the cathode – cylinder – collector geometry. Options with different locations of the anode mesh relative to the cylinder were also tested. The position of the mesh is determined by the position of the letter M mesh (mesh) in the CCC system (Fig. 11). Two meshes were also used at the beginning and at the end of the CMCMC cylinder.

It turned out that significantly larger beam currents, almost three times, are provided when using a dielectric cylinder without anode meshes, and it is conditioned by a decrease in electron losses on the anode.

2.5. BEAM POWER OF THE ELECTRON ACCELERATOR

Based on the obtained beam currents and voltages at the cathode-anode gap, it is possible to estimate the beam energy characteristics provided by the DIN-2K accelerator depending on the GIS charging voltage (Fig. 12). Two sets of data were obtained experimentally. The first set of data was obtained, when the beam current was measured by the beam collector that was located at the position of the anode mesh. The second set of data was obtained using a beam collector that was located behind the anode mesh at a distance of 30 mm from the anode mesh. The collector registers the maximum amplitude value of the oscillating current that passed through the virtual cathode (VC) region and after the VC region it began to accelerate in the self-consistent electromagnetic fields created in the drift chamber of the DIN-2K accelerator.

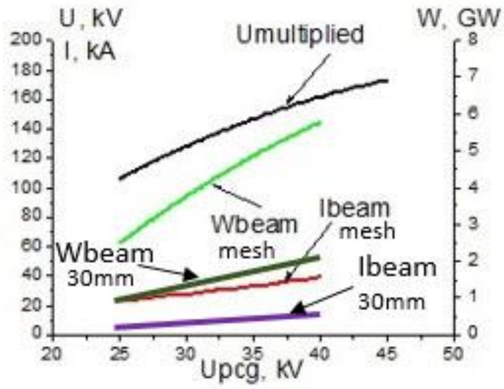

Fig. 12. Dependence of the beam power in the vacuum diode on the PCG charging voltage when the beam current is measured by the beam collector located at the position of the anode mesh and the power of the beam in the vacuum diode on the PCG charging voltage when the beam current is measured by the beam collector located at a distance of 30 mm from the anode mesh with registration of induced voltage

It can be seen from Fig. 12 that the beam power is increased with an increase in the PCG charging voltage, and it is related both to an increase in the beam current and the voltage in the cathode-anode gap. The maximum power values are achieved at a PCG charging voltage of 40 to 45 kV and an induced voltage of about 200 kV.

CONCLUSIONS

The DIN-2K electron accelerator with IES and POS has been upgraded to increase the current and beam power.

Cathodes of various geometries made of copper, steel, and graphite, were experimentally investigated in order to obtain maximum beam currents. It has been experimentally shown that the diameter of the cathode should be 1.5 to 3 times smaller than the diameter of the anode. Cathodes close in size to the anode are ineffective due to the mismatch of the impedance of the vacuum diode with the coaxial waveguide. In addition, beam losses from such cathodes on the side surface of the camera are disproportionately large. Cathodes with a diameter 5 to10 times smaller than the diameter of the anode are not effective due to the insignificant plane of the emitting surface. The largest beam current of 13.6 kA at voltages of 40 to 45 kV was obtained from a gear-shaped cathode. Electrodes made of stainless steel, copper and carbon are similar in their emitting capabilities, and the currents varying in the range of 5 to 11 kA were obtained from them, depending on the initial GIS charging voltage. In the range of charging voltages varying from 30 to 40 kV, the approximation curves for cathodes made of three types of materials have no significant differences in values.

After opening the plasma switch, the maximum voltage values are 187 kV for the DIN-2K accelerator. The voltage multiplication factor is K = 5.2.

The maximum beam current in the vacuum diode is 32.5 kA at a voltage for the GIS capacitor bank of 45 kV, provided that the beam collector is located on the anode mesh.

The largest beam current of 13.6 kA, at voltages of 40 to 45 kV, was obtained from the gear-shaped cathode, when recording the current behind the anode mesh.

It was established that the geometry of the cathode has an effect on the coherence of the wave resistances of the transmission coaxial line and the vacuum diode. The visual inspection of spent cathodes shows that the electron emission occurs mainly from the end surface and places with sharp edges.

A dielectric focusing lens made of porcelain is optimal. It is tightly pressed to the anode and has an internal diameter of 65 mm that reduces the losses of beam electrons on the side surface of the vacuum chamber. At the same time, the beam current was increased to 26 at 40 kV on the PCG at a distance of 30 mm from the anode mesh

Beam currents and voltages in the cathode-anode gap make it possible to estimate the power of the beam provided by the DIN-2K accelerator depending on the PCG charging voltage. The maximum power of the beam in the vacuum diode is estimated based on the measured current and energy, and its value is equal up to 6 GW. Based on the measured current and energy, the estimated power of the beam at a distance of 30 mm from the anode mesh in the DIN-2K accelerator chamber is up to 2 GW. The indicated capacities are sufficient for the fulfillment of multifunctional scientific and technical tasks.

REFERENCES

1. D.V. Vinnikov, V.V. Katrechko, O.M. Ozerov, V.I. Tkachev, S.V. Marchenko V.B. Yuferov, O.V. Manuilenko. Influence of the Energy Parameters of the Primary Circuit on the Current Characteristics of the Din-2k Accelerator // *Problems of Atomic Science and Technology. Series "Plasma Electronics and New Methods of Acceleration"*. 2023, N 4 p. 36-40; https://doi.org/10.46813/2023-146-036

2. D.V. Vinnikov, V.V. Katrechko, O.M. Ozerov, V.I. Tkachev, S.V. Marchenko, V.B. Yuferov, O.V. Manuilenko. Influence of the energy parameters of the primary circuit on the current characteristics of the DIN-2K accelerator // *Oral paper at XVI International Workshop "Plasma Electronics and New Methods of Acceleration",* September 5-6, 2023, Kharkov, Ukraine: Book of Abstracts, p. 12; https://kipt.kharkov.ua/conferences/ipenma/2023/First_Announcement_IW_PENMA_2023.pdf https://kipt.kharkov.ua/conferences/ipenma/2023/Abstracts.pdf

3. В.Б. Юферов, О.В. Мануйленко, Д.В. Вінніков, В.В. Катречко, О.М. Озеров, В.І. Ткачьов, С.В. Марченко, В.В. Єгоренков, В.Т. Фомін. Вплив часу затримки між розрядами плазмових гармат та основного ГІСу на комутацію струму в прискорювачах з індуктивним накопичувачем енергії та плазмовим комутатором струму // *Тези доповідей XXI Конференції з фізики високих енергій та ядерної фізики* (21–24 березня 2023); https://www.kipt.kharkov.ua/conferences/ihepnp/2023/rep_XXI_conf_ukr.pdf

4. O.S. Druj, V.V. Yegorenkov, I.M. Onyshchenko, V.B. Yuferov. Plasma Dynamics in Accelerator with Plasma Opening Switch // *Problems of Atomic Science and Technology.* 2019, N 6(124), p. 77-80; https://doi.org/10.46813/2019-124-077

5. O.S. Druj, V.V. Yegorenkov, A.V. Shchagin, V.B. Yuferov. Electron beam transport in dielectric tubes // *East European Journal of Phisics*. 2014, v. 1, N 1, p. 70-73.

6. O.V. Manuilenko, I.N. Onishchenko, A.V. Pashchenko, I.A. Pashchenko, V.B. Yuferov. Current Flow Dynamics in Plasma Opening Switch // *Problems of Atomic Science and Technology.* 2021, N 4(134), p. 6-10; https://doi.org/10.46813/2021-134-006

7. S.V. Loginov. Conduction Current in Low-Density Plasma Opening Switches // *IEEE Transactions on Plasma Science.* 2022, N 50(7), p. 2026-2029; https://doi.org/10.1109/TPS.2022.3178792

8. James Benford, John A. Swegle, Edl Schamiloglu. *High Power Microwaves*. CRC Press, 2015, 447 p.

9. O.V. Manuilenko, I.N. Onishchenko, A.V. Pashchenko, I.A. Pashchenko, V.A. Soshenko, V.G. Svi-

chensky, V.B. Yuferov, B.V. Zajtsev. Magnetic Field Dynamics in Plasma Opening Switch // *Problems of Atomic Science and Technology*. 2021, N 6(136), p. 61-66; https://doi.org/10.46813/2021-136-061

10. O.V. Manuilenko, I.N. Onishchenko, A.V. Pashchenko, I.A. Pashchenko, V.B. Yuferov. Plasma and Magnetic Field Dynamics in POS: PIC simulations // *Problems of Atomic Science and Technology*. 2022, N 6(142), p. 55-59; https://doi.org/10.46813/2022-142-055

11. D.V. Vinnikov, V.V. Katrechko, V.B. Yuferov, V.I. Tkachev. Plasma Guns of an Erosion Type with the Pulse-Periodic Gas-Metal Injection // *Problems of Atomic Science and Technology*. 2022, N 6(142), p. 60-65; https://doi.org/10.46813/2022-142-060

12. Y.Y. Lau. Simple Theory for the Two-Dimensional Child-Langmuir Law // *Physical Review Letters*. 2001, v. 87, N 27, p. 278301.

13. J.W. Luginsland, Y.Y. Lau, R.M. Gilgenbach. Simple Two-Dimensional Child-Langmuir Law // *Physical Review Letters*. 1996, v. 77, N 22, p. 4668-4670.

Article received 30.04.2024

ПІДВИЩЕННЯ ФУНКЦІОНАЛЬНОСТІ МАЛОГАБАРИТНОГО ПРИСКОРЮВАЧА ДІН-2К З ПЛАЗМОВИМ РОЗМИКАЧЕМ

Д.В. Вінніков, В.В. Катречко, О.В. Мануйленко, О.М. Озеров, І.М. Оніщенко, В.І. Ткачов, В.Б. Юферов, С.В. Марченко

Проведено експериментальні дослідження впливу параметрів різних вузлів електронного прискорювача з ІНЕ та ПКС на струм та потужності прискореного пучка. Дослідження включали підбір співвідношення параметрів розрядного контуру ІНЕ, геометричної форми і матеріалу катода, величини анод-катодного зазору і діелектричних вставок. Знайдено оптимальний набір зазначених параметрів, що дозволив отримати імпульсний електронний пучок тривалістю 200 нс, струмом 30 кА і потужністю 6 ГВт.